Volume 1 | Number 1 | Jan 2013 | Pages 1–100
RSC Advances
www.rsc.org/advances
ROYAL SOCIETY OF CHEMISTRY

Journal Name RSCPublishing

COMMUNICATION

Sodium alginate assisted photosynthesis of silver complex microarchitectures

Cite this: DOI: 10.1039/x0xx00000x

Received 00th January 2012,
Accepted 00th January 2012

DOI: 10.1039/x0xx00000x

www.rsc.org/

Man Guan, Zhimin Zhou,* Ruiping Duan, Bo Du, Xuemin Li, Lingrong Liu and Qiqing Zhang*

Silver flower-like complex polycrystalline microarchitectures were synthesized in the presence of sodium alginate, facilitated by oriental adherence of polysaccharide under natural light. These 3D microarchitectures displayed unique SPR absorption, as well as the significant Raman scattering activity.

Self-organization of complex structures from colloidal particles is a significant synthetic method to obtain multi-functional materials.[1, 2] Ag dendritic or flower-like microstructures, known as one intensively studied category of such complex structures, have attracted great attentions due to their distinct features.[3-5] Moreover, most of these specific microstructures formation usually obeys the underlying principle of diffusion-limited aggregation (DLA) process or oriented attachment.[5-7] Recently, biomolecules were utilized to induce self-organization of metal particles. Biotin was reported to apply on synthesis of fiber-like microstructures from Ag spherical particles, owing to its tunable weak interactions with silver ions.[8] Similarly, salep, another common biomolecule, could also contribute to Ag flower-like microarchitectures assembly from wedge-like particles under sunlight irradiation.[3] Such exciting achievements inspired us to develop Ag complex architectures using biomolecules and energy-saving natural light for potential biomedical purposes.

Here we reported a new biomolecule-assisted approach to induce organization of Ag complex microarchitectures. Sodium alginate (SA), a biocompatible natural polysaccharide, which has active metal-binding sites arising from carboxylate groups,[9] was mixed with $AgNO_3$. The mixture was then irradiated with natural light for 1 h (400 - 700 lux horizontal illuminance). The color of the solution was changed from initial colorless to crimson appearance (see ESI,† Fig. S1). This solution was directly dropped on TEM grid, and the typical flower-like particles with ca. 3.8 μm of cores was observed (Fig. 1a). Branches, forming the corona of microarchitectures, are 240 nm in the mean diameter, and 4.3 μm in length, respectively. The core-corona structure is similar to the schematic illustration of self-assembled polymeric micelles.[10] Close inspection of individual complex architecture (Fig. 1b) revealed that

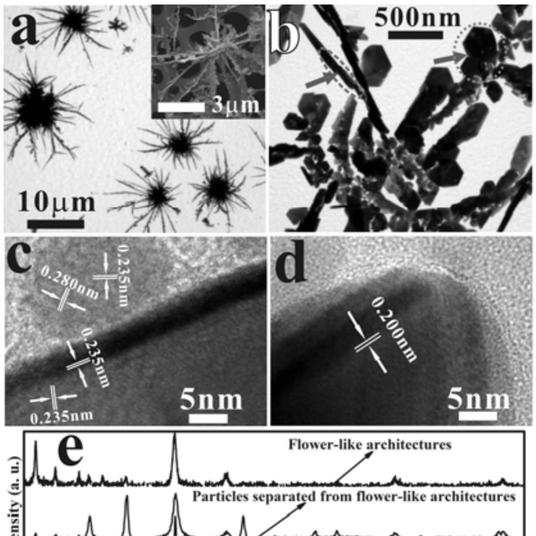

Fig. 1 TEM (a, b), HRTEM (c, d) and SEM (a inset) images of flower-like complex microarchitectures. e, XRD patterns of different particles. SA, 0.5 %; $AgNO_3$, 0.1 %; Natural light irradiation, 1h.

it consisted of plate-like particles, which were ca. 460 nm in length and ca. 70 nm in thickness, respectively. More interesting, it is clear that part of plates were perpendicular to the substrate, which is in agreement with SEM images (Fig. 1a inset, also see ESI,† Fig. S2). The 3D structure arising from upright plates offers a distinct advantage for SERS detection due to the enhanced active surface for absorbing more molecules than flat counterparts.[11] On the other hand, it seemed that these nanoplates were adhered to each other via plate by plate orderly as indicated by arrows in Fig. 1b. However, the complex microarchitectures were destroyed after treating as-synthesized solution by centrifugation. Instead of complex structures, independent plate-like particles were obtained and the mean size was comparable before and after separation (see ESI,† Fig. S3a). Therefore, considering the low stability, the formation of such complex structure, is likely weak interaction driven nanoplates organization than traditional crystal growth of dendrites.[6, 7]

Actually, high-resolution TEM images (Fig. 1c and d) showed that the complex architectures were composed of AgCl and Ag. The lattice spacing of 0.280 is indexed to (200) plane of AgCl, however, the measured lattice spacing of 0.235 nm and 0.200 nm corresponds to (111) and (200) planes of face-centered cubic (FCC) Ag, respectively. Since the lattice orientation was obvious difference between Ag and AgCl block, the branches of microarchitecture must not be epitaxial growth from the stem.[5, 7, 12] The polycrystalline structure of architectures was further confirmed by the corresponding selected area electron diffraction pattern (see ESI,† Fig. S3b), which is in accordance with TEM and HRTEM analysis (Fig. 1b-d). The appearance of AgCl was also confirmed by XRD. As shown in Fig. 1e, besides the typical peaks of cubic metal silver (JCPDF No. 04-0783)[5, 7], the diffraction peak located at 32.2° was assigned to (200) crystal plane of AgCl (JCPDF No. 31-1238).[12,13] After centrifugation, the diffraction peaks intensity of AgCl became stronger, which could be ascribed to the removal of impurities including NaAgO (JCPDF No. 01-077-1695) and $AgClO_3$ (JCPDF No. 01-075-0886) by washing.

Previously, most of the reported Ag flower-like structures were attributed to DLA or oriented attachment, and few of them involved Cl^-.[5, 7] In our system, the residual Cl in commercially available SA of ca. 2.5 g / kg was detected using ion chromatography. To verify the role of Cl ions on the formation of these complex composite microarchitectures, a control experiment was conducted using Cl^- removed SA by dialysis. In comparison with the commercial SA, Cl^- removed SA led changes in both color (from colorless transparent to greenish-gray, see ESI,† Fig. S4) and time consumption (8 h). Further TEM characterization showed that most of particles of ca. 23 nm are spherical in shape (Fig. 2a). The diffraction peaks of XRD pattern of the spherical particles could be indexed to the corresponding (111), (200), (220) and (311) crystal planes for FCC phase silver with negligible AgCl signals (Fig. 1e).[5, 7] Previously, it was proposed that Cl ions can not only guide anisotropic growth but also perform shape transformation of silver nanoparticles.[14, 15] Moreover, AgCl could be photoconverted to functional silver nanoparticles.[16] Therefore, we consider that Cl ions, in the form of AgCl, play a pivotal role to induce flower-like complex architectures formation.

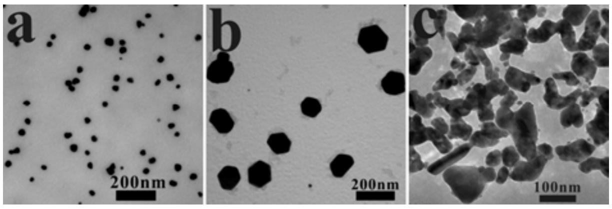

Fig. 2 TEM images of photosynthesized Ag nanoparticles employing different polysaccharides (0.5 %). a, purified SA with Cl^- removal, 8h; b, chitosan, 1h; c, SA, 30min. $AgNO_3$, 0.1 %.

Besides Cl^-, SA is likely to be another key factor affecting the formation of complex architectures. Using other commercially available natural polysaccharides including chitosan, carboxymethylcellulose, soluble starch to replace SA in the system, only dispersive particles were yielded without any complex assemblies (Fig. 2b, also see ESI,† Fig. S5). Moreover, we also tracked the shape transition from spherical particles to nanoplates when irradiated for 30 min. (Fig. 2c), indicated particles evolution under natural light over time.[17]

Scheme 1 Photosynthesis of Ag complex microarchitectures through order adherence of nanoplates using sodium alginate (SA) followed by self-organization of branches. LWL, long-wavelength light.

Based on the above results, the formation mechanism of complex microarchitectures was clarified in scheme 1. First, trace of

Cl^- reacted with Ag^+ to produce AgCl crystal nucleus, which absorbed photons, released electron to reduce Ag^+ to Ag seeds.[13, 16] Then, under irradiation with natural light, such Ag seeds continued growth, and further converted into anisotropic nanoplates because of the long-wavelength excitation effect.[17] The (111) plane of as-converted AgCl / Ag nanoplates was known to absorb SA. The absorbed SA on (111) plane not only accelerated the growth of nanoplates via chelating silver ions by carboxyl groups, but also induced nanoplates adherence one by one erectly, which contributed final complex architectures formation via branches self-organization.

Finally, the optical properties of as-synthesized complex architectures were characterized for their potential biomedical applications. As shown in Fig. 3a, the single UV absorption band of spherical particles was located at ca. 410 nm, which is in agreement with previous literature for Ag particles.[17, 18] However, the spectrum of flower-like architectures showed an additional absorption band at ca. 969 nm compared to that of mixed particles after centrifugation, which can be ascribed to the aggregation of metal particles.[17] The localized surface plasmon resonance adsorption in the NIR region suggested that the complex architectures are likely to contribute Raman scattering enhancement.[18] In fact, silver flower-like architectures displayed significant Raman scattering activity in comparison with quartz or silver nanospheres substrates using crystal violet (2×10^{-6} M) as Raman tag (Fig. 3b). We considered that both size and 3D geometry of flower-like complex particles played an important role in the enhancement as the localized surface plasmon coupling and the enhanced electromagnetic field intensity provided useful features for SERS detection.[4, 11, 17]

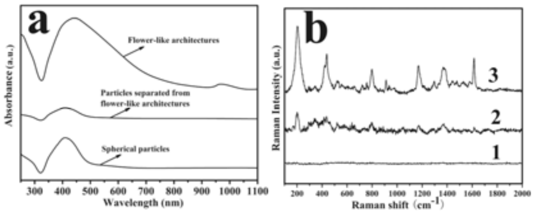

Fig. 3 a, Uv-vis spectra of flower-like microarchitectures, particles separated from flower-like architectures by centrifugation and Ag nanospheres (from top to down). b, Raman spectra of crystal violet (2×10^{-6} M) on different substrates. 1, quartz; 2, silver nanospheres; 3, flower-like microarchitectures.

In summary, Ag flower-like complex polycrystalline microarchitectures with distinct optical features were reported. The Cl^- and SA served as unique assistant reagents to induce plate-by-plate adherence. This simple methodology could be potential applied to other systems involved different nanopaticles. Also, the 3D microstructures have promising applications for biomedical detection and photocatalysis.

This work was supported by the Major Research Plan of NSFC (91323104) & NSFC (31271023, 31170917), the PUMC Youth Fund (33320140054) & the Fundamental Research Funds for the Central Universities, and the Basic Research Fund of State Institutes for Public Career.

Notes and references

Institute of Biomedical Engineering, Chinese Academy of Medical Sciences & Peking Union Medical College, the Key Laboratory of Biomedical Material of Tianjin, Tianjin 300192, P.R. China. E-mail:zhouzm@bme.cams.cn; zhangqiq@126.com

†Electronic Supplementary Information (ESI) available: See DOI: 10.1039/c000000x/

1 S. C. Glotzer and M. J. Solomon, *Nat. Mater.*, 2007, **6**, 557-562.
2 M. Grzelczak, J. Vermant, E. M. Furst and L. M. Liz-Marzan, *ACS Nano*, 2010, **4**, 3591-3605.
3 A. Pourjavadi and R. Soleyman, *Mater. Res. Bull.*, 2011, **46**, 1860-1865.
4 K. A. Homan, J. Chen, A. Schiano, M. Mohamed, K. A. Willets, S. Murugesan, K. J. Stevenson and S. Emelianov, *Adv. Funct. Mater.*, 2011, **21**, 1673-1680.
5 X. Wen, Y. T. Xie, M. W. Mak, K. Y. Cheung, X. Y. Li, R. Renneberg and S. Yang, *Langmuir*, 2006, **22**, 4836-4842.
6 J. A. Corno, J. Stout, R. Yang and J. L. Gole, *J. Phys. Chem. C*, 2008, **112**, 5439-5446.
7 L. Lu, A. Kobayashi, Y. Kikkawa, K. Tawa and Y. Ozaki, *J. Phys. Chem. B*, 2006, **110**, 23234-23241.
8 S. Hegde, S. Kapoor, S. Joshi and T. Mukherjee, *J.Colloid Interf. Sci.*, 2006, **297**, 637-643.
9 L. Meng, W. Xia, L. Liu, L. Niu and Q. Lu, *ACS Appl. Mater. Inter.*, 2014, **6**, 4989-4996.
10 J. Rodríguez-Hernández, F. Chécot, Y. Gnanou and S. Lecommandoux, *Prog. Polym. Sci.*, 2005, **30**, 691-724.
11 B. B. Xu, L. Wang, Z. C. Ma, R. Zhang, Q. D. Chen, C. Lv, B. Han, X. Z. Xiao, X. L. Zhang, Y. L. Zhang, K. Ueno, H. Misawa and H. B. Sun, *ACS Nano*, 2014, **8**, 6682-6692.
12 M. Choi, K.-H. Shin and J. Jang, *J.Colloid Interf. Sci.*, 2010, **341**, 83-87.
13 P. Wang, B. Huang, X. Qin, X. Zhang, Y. Dai, J. Wei and M. H. Whangbo, *Angew. Chem.-Int. Edit.*, 2008, **47**, 7931-7933.
14 B. Wiley, T. Herricks, Y. Sun and Y. Xia, *Nano Lett.*, 2004, **4**, 1733-1739.
15 J. An, B. Tang, X. Zheng, J. Zhou, F. Dong, S. Xu, Y. Wang, B. Zhao and W. Xu, *J. Phys. Chem. C*, 2008, **112**, 15176-15182.
16 G. Wang, T. Nishio, M. Sato, A. Ishikawa, K. Nambara, K. Nagakawa, Y. Matsuo, K. Niikura and K. Ijiro, *Chem. Commun.*, 2011, **47**, 9426-9428.
17 K. G. Stamplecoskie and J. C. Scaiano, *J. Am. Chem. Soc.*, 2010, **132**, 1825-1827.
18 X. Cui, C. M. Li, H. Bao, X. Zheng, J. Zang, C. P. Ooi and J. Guo, *J. Phys. Chem. C*, 2008, **112**, 10730-10734.